Dielectronic-recombination cross sections and rate coefficients for S^{3+}

Abdulrahman Al-Mulhem and Ibraheem Nasser
Department of Physics, King Fahd University of Petroleum and Minerals, Dhahran 31261, Saudi Arabia
(Received 18 February 1992)

The dielectronic-recombination cross sections and rate coefficients of Al-like S^{3+} ion are calculated for the process in which the $3s$ electron is excited to the $3p$ state and the projectile electron is captured to a high Rydberg state (nl). The calculations have been done using single-configuration and nonrelativistic Hartree-Fock wave functions in LS coupling. The transitions from the ground state $(3s^2 3p)^2P$ and the multiplets of the first excited state $(3s3p^2)$ have been included explicitly. We tabulated our results of the cross sections and rate coefficients to facilitate direct comparison with future experimental data.

PACS number(s): 34.80.Kw, 34.80.Dp

Electron capture by ionic targets ($A^{z+}=i$) with a degree of ionization z via intermediate resonance states [$(A^{(z-1)+})^{**}=d$], followed by stabilizing radiation emission to a final state [$(A^{(z-1)+})^{*}=f$], is known as the dielectronic-recombination (DR) process [1,2]. It is an important tool by which astronomical and laboratory high-temperature plasmas cool radiatively. Accurate estimation of the rate coefficients of processes like DR for many different ions is essential to make precise descriptions of the behavior of such types of plasmas. There has been much interest in measuring the oxygen-to-sulfur ratio in Jupiter's plasma torus [3]. The method of measurement depends on ion emissions in the torus. Knowing the rate coefficients of the different ions involved is important to make acceptable measurements of the ratio. In more recent theoretical work done by Badnell [4] for S^{q+}, he used LS coupling incorporated with configuration mixing to the N-electron core. In this report we present our results of estimating DR cross sections and rate coefficients of Al-like S^{3+} for the process in which the $3s$ electron is excited to the $3p$ state and the projectile electron is captured to high Rydberg state (nl) using single-configuration and relativistic Hartree-Fock wave functions in the LS coupling scheme. The DR process could simply be represented in the $\Delta n=0$, $\Delta l=1$ mode of excitation by

$$(3s^2 3p=i)+k_c l_c \rightarrow (3s3p^2 nl=d) \rightarrow (3s3p^2 n'l'=f)+\gamma(nl\rightarrow n'l') \quad (1)$$

with an extra Auger channel $\Delta n=0$, $\Delta l=0$ mode due to the multiplets of the first excited state $(3s3p^2)$, i.e.,

$$(3s3p^2=i')+k_c' l_c' \rightarrow (3s3p^2 nl=d) \rightarrow (3s3p^2 n'l'=f)+\gamma(nl\rightarrow n'l') \; . \quad (2)$$

(Explicit reference to the core electrons and multiplets of the excited states of Al-like ions is omitted for simplicity.)

The details of the theoretical method employed in this work will not be presented here as such. They are fully covered in previous works by Hahn [1] and Hahn and LaGattuta [2].

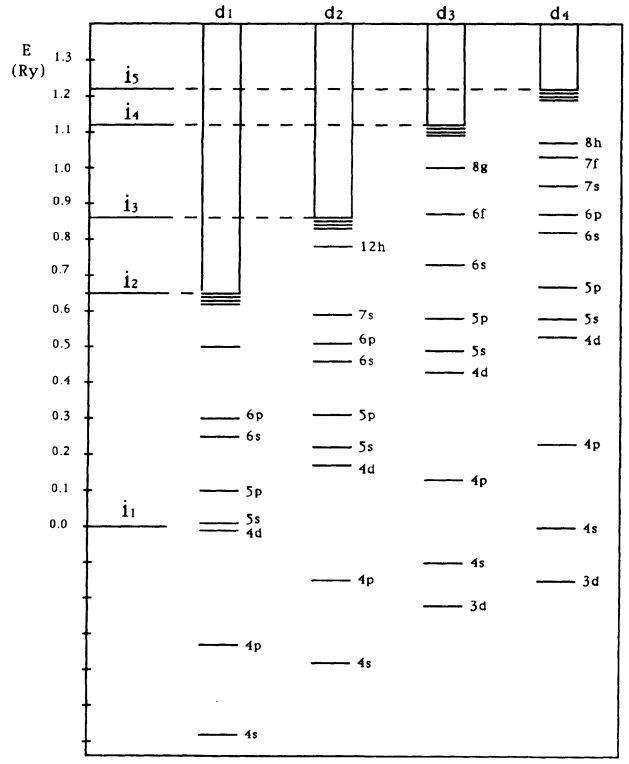

FIG. 1. Energy-level diagram of S^{3+} ion showing relevant levels to DR process, from which all possible radiative and Auger transitions for the individual intermediate resonance states may be determined.

TABLE I. Energy differences of S^{3+} ionic cores and their dominant radiative decay rates A_r. The numbers in brackets represent powers of 10.

i	ΔE (Ry)	A_r (sec^{-1})
$i_1=(3s^2 3p)^2P$	0	0
$i_2=(3s3p^2)^4P$	0.652	0
$i_3=(3s3p^2)^2D$	0.858	1.43[+09]
$i_4=(3s3p^2)^2S$	1.130	3.08[+09]
$i_5=(3s3p^2)^2P$	1.220	1.20[+10]

We used Cowan's code [5] in single-configuration and nonrelativistic Hartree-Fock approximations and in the *LS* coupling scheme in the evaluation of the transition energies, as well as the relevant A_a Auger emission probability and A_r radiative transition probability used in the estimation of the DR cross sections. Data tables [6] were consulted to adjust energies, wherever possible.

For convenience, we define the various channels needed in our work as

$$i_1=(3s^23p)^2P\ ,$$

$$i_2=(3s3p^2)^4P\ ,\quad d_1=(i_2)nl\ ,$$

$$i_3=(3s3p^2)^2D\ ,\quad d_2=(i_3)nl\ ,$$

$$i_4=(3s3p^2)^2S\ ,\quad d_3=(i_4)nl\ ,$$

$$i_5=(3s3p^2)^2P\ ,\quad d_4=(i_5)nl\ .$$

In Fig. 1 the energy levels relevant to the DR process for the S^{3+} ion are given, from which all possible radiative and Auger transitions for the individual intermediate resonance states may be determined. Energy differences and the radiative transition probabilities of the ionic core involved are shown in Table I, and these are the dominant radiative decay rates for large n. The cross sections $\bar{\sigma}^{\rm DR}$ (cm^2) as functions of electron energies e_c (Ry) for the ground state i_1 are tabulated in Table II, and the explicit contributions of each intermediate-state series are also given. Cross sections $\bar{\sigma}^{\rm DR}$ (cm^2) for the initial states i_2,

TABLE II. DR cross sections $\bar{\sigma}^{\rm DR}$ (cm^2) as functions of electron energies e_c (Ry) for the ground state i_1, with $\Delta e_c=0.02$ Ry. Explicit contributions from the intermediate states d_1, d_2, d_3, and d_4 are given. The numbers in brackets represent powers 10.

e_c	^4P	^2D	^2S	^2P
0.06	9.80[−20]			
0.10	8.65[−21]			
0.16		1.46[−19]		
0.20		3.61[−20]		
0.22	1.48[−21]			
0.24	2.36[−21]			
0.26	1.44[−20]	2.09[−19]		
0.30	1.67[−21]	4.28[−20]		
0.36	1.20[−21]			
0.38	6.91[−21]			
0.44	5.25[−22]	4.31[−20]	1.74[−20]	
0.46	3.80[−21]	1.20[−20]		
0.48	1.34[−25]	1.42[−19]	4.77[−21]	
0.50	2.90[−21]	2.44[−20]		
0.52	1.73[−21]			1.70[−19]
0.54	1.52[−21]		2.85[−20]	
0.56	1.66[−21]	3.32[−20]		3.91[−20]
0.58	1.16[−21]	1.61[−20]	2.45[−21]	
0.60	1.22[−21]	1.81[−19]		
0.62	9.56[−22]			2.56[−19]
0.64		1.92[−20]		
0.66		2.07[−19]		7.75[−20]
0.68				
0.70		2.41[−19]	7.00[−21]	
0.72		2.78[−20]	2.42[−21]	
0.74		3.09[−19]		
0.76		3.04[−19]	3.73[−20]	
0.78		8.33[−19]		
0.80		1.90[−18]		9.80[−20]
0.82		4.81[−18]		2.36[−20]
0.84		1.04[−17]	7.15[−21]	3.27[−19]
0.86			1.56[−20]	5.50[−20]
0.88			7.90[−21]	
0.90				
0.92			2.76[−21]	9.15[−20]
0.94			3.06[−20]	1.93[−20]
0.96			1.84[−21]	4.77[−19]
0.98			4.12[−20]	
1.00			1.09[−20]	4.30[−20]
1.02			5.54[−20]	6.25[−19]
1.04			1.42[−19]	3.80[−20]
1.06			2.50[−19]	1.68[−19]
1.08			8.39[−19]	6.54[−19]
1.10			2.52[−18]	9.50[−19]
1.12			5.15[−19]	1.12[−18]
1.14				2.69[−18]
1.16				3.82[−18]
1.18				1.19[−17]
1.20				2.70[−19]
Total	1.50[−19]	1.99[−17]	4.55[−18]	5.15[−17]

TABLE III. DR cross sections $\bar{\sigma}^{\rm DR}$ (cm^2) as functions of electron energies e_c (Ry), with $\Delta e_c=0.02$ Ry for the excited states i_2, i_3, and i_4. The numbers in brackets represent powers of 10.

e_c	^4P	^2D	^2S
0.01	2.48[−19]	6.48[−19]	1.00[−18]
0.03			8.88[−19]
0.05	1.06[−19]	3.66[−20]	5.79[−18]
0.07	3.91[−20]	3.14[−19]	4.18[−18]
0.09	7.10[−20]	4.81[−20]	
0.11	7.51[−20]	6.67[−20]	
0.13	1.59[−19]	1.65[−19]	
0.15	1.78[−18]	2.77[−19]	
0.17	2.01[−18]	2.55[−19]	
0.19	6.45[−19]	4.00[−19]	
0.21	1.26[−20]	9.10[−19]	
0.23	7.60[−22]	1.97[−18]	
0.25		5.75[−18]	
0.27	2.06[−20]	1.26[−19]	
0.29	2.65[−21]	1.74[−19]	
0.31	1.39[−20]	1.18[−18]	
0.33	9.03[−22]	2.09[−18]	
0.35	1.59[−21]	1.98[−18]	
0.37	1.33[−20]		
0.39	4.47[−21]		
0.41	2.25[−20]		
0.43	9.87[−19]		
0.45	1.89[−19]		
0.47	2.58[−20]		
0.49	6.15[−20]		
0.51	2.86[−19]		
0.53	5.52[−19]		
0.55	1.17[−19]		

TABLE IV. Rate coefficients $\bar{\alpha}^{DR}$ (cm^3/sec) as functions of kT (Ry) for the ground state i_1 are compared with those obtained by Badnell [4] and Jacobs *et al.* [9]. The numbers in brackets represent powers of 10.

kT (Ry)	^4P	^2D	^2S	^2P	Total	Badnell	Jacobs
0.10[+00]	0.65[−12]	0.23[−11]	0.43[−13]	0.21[−12]	3.2[−12]		4.9[−12]
0.20[+00]	0.42[−12]	0.16[−10]	0.12[−11]	0.99[−11]	2.8[−11]	2.9[−11]	1.0[−11]
0.25[+00]	0.36[−12]	0.25[−10]	0.25[−11]	0.22[−10]	5.0[−11]	4.8[−11]	3.8[−11]
0.30[+00]	0.31[−12]	0.32[−10]	0.39[−11]	0.36[−10]	7.2[−11]	7.7[−11]	8.5[−11][a]
0.39[+00]	0.25[−12]	0.40[−10]	0.61[−11]	0.60[−10]	1.1[−10]	1.1[−10]	1.0[−10]
0.50[+00]	0.19[−12]	0.43[−10]	0.77[−11]	0.80[−10]	1.3[−10]	1.4[−10]	1.4[−10][a]
0.60[+00]	0.16[−12]	0.43[−10]	0.85[−11]	0.90[−10]	1.4[−10]	1.6[−10]	1.6[−10]
0.79[+00]	0.12[−12]	0.40[−10]	0.87[−11]	0.95[−10]	1.5[−10]	1.6[−10]	1.7[−10][a]
0.99[+00]	0.91[−13]	0.35[−10]	0.82[−11]	0.92[−10]	1.4[−10]	1.6[−10]	1.6[−10]
0.12[+01]	0.71[−13]	0.30[−10]	0.75[−11]	0.85[−10]	1.2[−10]	1.4[−10]	1.5[−10][a]
0.16[+01]	0.49[−13]	0.24[−10]	0.61[−11]	0.71[−10]	1.0[−10]	1.2[−10]	1.3[−10]
0.20[+01]	0.37[−13]	0.19[−10]	0.50[−11]	0.59[−10]	8.3[−11]	1.0[−10]	1.1[−10][a]
0.25[+01]	0.27[−13]	0.15[−10]	0.40[−11]	0.47[−10]	6.6[−11]	8.0[−11]	8.7[−11]
0.31[+01]	0.20[−13]	0.11[−10]	0.32[−11]	0.37[−10]	5.1[−11]	6.3[−11]	7.0[−11][a]
0.39[+01]	0.14[−13]	0.84[−11]	0.24[−11]	0.29[−10]	4.0[−11]	4.8[−11]	5.2[−11]
0.50[+01]	0.10[−13]	0.61[−11]	0.18[−11]	0.21[−10]	2.9[−11]	3.6[−11]	4.1[−11][a]
0.63[+01]	0.73[−14]	0.44[−11]	0.13[−11]	0.16[−10]	2.2[−11]	2.7[−11]	2.9[−11]
0.80[+01]	0.51[−14]	0.32[−11]	0.95[−12]	0.11[−10]	1.5[−11]		1.6[−11]
0.10[+02]	0.37[−14]	0.23[−11]	0.70[−12]	0.84[−11]	1.1[−11]		
0.12[+02]	0.28[−14]	0.18[−11]	0.54[−12]	0.65[−11]	8.8[−12]		

[a]These figures were extrapolated.

i_3, and i_4 as functions of e_c (Ry) are tabulated in Table III. It is important to estimate the contributions from excited states [7] even though some states are not able to radiatively stabilize such as i_3 and i_4, but the metastable state i_2 is usually present in the ion beam with unknown percentage (perhaps 50%) [8]. As shown in Table III, the contribution of the metastable state i_2 is about 10% of i_1, and this may affect the overall distribution of the rates and cross sections at small values of e_c, $e_c \leq 0.55$ Ry. In $\Delta n = 0$, $\Delta l = 1$ mode we compared our results for the rate coefficients with those given by Badnell [4] and Jacobs *et al.* [9] in Table IV and it was found that our results as well as those of Badnell and Jacobs peak at $kT = 0.79$ (Ry), which is $\frac{2}{3}$ of the energy gap between i_1 and i_5. This peak is mainly due to d_2 and d_4 series. There is a factor of 1.08 of Badnell [4] results to ours at the temperature of the peak. This difference may be due to the configuration mixing he used in the core. Although Jacobs *et al.* [9] imposed a cutoff on n given by the Inglis-Teller criteria, his results are 1.13 times larger than our results. This is because he neglected the nondipole

TABLE V. Rate coefficients $\bar{\alpha}^{DR}$ (cm^3/sec) as functions of kT (Ry) for the excited states i_2, i_3, and i_4. The numbers in brackets represent powers of 10.

kT (Ry)	^4P	^2D	^2S
0.40[−02]	9.1[−13]	1.9[−12]	3.2[−12]
0.60[−02]	2.4[−12]	5.0[−12]	6.9[−12]
0.80[−02]	3.5[−12]	7.2[−12]	1.0[−11]
0.10[−01]	4.1[−12]	8.5[−12]	1.5[−11]
0.30[−01]	5.8[−12]	9.4[−12]	7.3[−11]
0.50[−01]	1.2[−11]	1.6[−11]	8.6[−11]
0.80[−01]	2.1[−11]	3.3[−11]	7.3[−11]
0.10[+00]	2.4[−11]	4.2[−11]	6.2[−11]
0.30[+00]	1.8[−11]	4.5[−11]	2.0[−11]
0.50[+00]	1.2[−11]	3.0[−11]	1.0[−11]
0.80[+00]	7.6[−12]	1.8[−11]	5.3[−12]
0.10[+01]	5.8[−12]	1.4[−11]	3.8[−12]
0.30[+01]	1.4[−12]	3.3[−12]	7.8[−13]
0.50[+01]	6.7[−13]	1.6[−12]	3.6[−13]
0.80[+01]	3.5[−13]	7.9[−13]	1.8[−13]
0.10[+02]	2.4[−13]	5.8[−13]	1.3[−13]
0.12[+02]	1.9[−13]	4.4[−13]	9.9[−14]
0.15[+02]	1.4[−13]	3.1[−13]	7.1[−14]

TABLE VI. DR cross sections $\bar{\sigma}^{DR}$ (cm^2) as functions of n in $\Delta n = 0$, $\Delta l = 1$ mode of excitation for the ground state i_1, with $\Delta e_c = 0.01$ Ry. The numbers in brackets represent powers of 10.

n	^4P	^2D	^2S	^2P
4	1.96[−19]	7.09[−19]	9.18[−20]	8.52[−19]
5	4.89[−20]	5.27[−19]	9.32[−20]	1.08[−18]
6	2.09[−20]	4.61[−19]	6.92[−20]	1.20[−18]
7	1.01[−20]	4.77[−19]	6.74[−20]	1.45[−18]
8	6.02[−21]	5.03[−19]	8.60[−20]	1.62[−18]
9	3.96[−21]	5.87[−19]	1.08[−19]	1.90[−18]
10	2.78[−21]	5.60[−19]	1.29[−19]	1.83[−18]
11–15	6.00[−21]	2.54[−18]	7.15[−19]	8.28[−18]
16–20	3.00[−21]	2.22[−18]	6.40[−19]	7.20[−18]
21–25	1.00[−21]	2.02[−18]	5.50[−19]	6.20[−18]
26–30		1.70[−18]	4.70[−19]	5.50[−18]
31–40		3.10[−18]	7.80[−19]	9.30[−18]
41–50		2.50[−18]	6.10[−19]	7.60[−18]
51–60		2.00[−19]	5.00[−19]	6.30[−18]
61–70		1.90[−18]	4.40[−19]	5.50[−18]
71–80		1.60[−18]	3.80[−19]	4.60[−18]
81–90		1.50[−18]	3.30[−19]	4.00[−18]
91–100		1.30[−18]	3.00[−19]	3.50[−18]
100–∞	0	1.33[−17]	2.63[−18]	2.51[−17]

autoionization, which when included will increase the total width of the intermediate state, i.e., will decrease their cross sections and rates by 15%. DR rate coefficients $\bar{\alpha}^{DR}$ (cm^3/sec) as functions of kT (Ry) for multiplet transitions are tabulated in Table V. For convenience, multiplet transition DR cross sections $\bar{\sigma}^{DR}$ (cm^2) in the $\Delta n=0$, $\Delta l=1$ mode of excitation are given in Table VI as functions of n.

Finally, we can conclude that the configuration mixing of the ion core is small for this ion, i.e., S^{3+}, and also the contribution of the metastable state i_2 could affect the overall distribution at small e_c, $e_c \leq 0.55$ Ry.

This work was carried out at KFUPM computer center using Cowan's atomic structure code. We would like to thank Dr. Badnell for sending his paper (Ref. [4]) to us.

[1] Y. Hahn, Adv. At. Mol. Phys. **21**, 123 (1985).
[2] Y. Hahn and K. LaGattuta, Phys. Rep. **166**, 195 (1988).
[3] D. E. Shemansky, J. Geophys. Res. **92**, 6141 (1988).
[4] N. R. Badnell, Astrophys. J. **379**, 356 (1991).
[5] R. D. Cowan, *The Theory of Atomic Structure and Spectra* (University of California Press, Berkeley, 1981).
[6] S. Bashkin and J. O. Stoner, Jr., *Atomic Energy Levels and Grotrian Diagrams* (North-Holland, Amsterdam, 1977).
[7] I. Nasser and Y. Hahn, Phys. Rev. A **44**, 6133 (1991).
[8] P. F. Dittner, S. Datz, R. Hippler, H. F. Krause, P. D. Miller, P. L. Pepmiller, C. M. Fou, Y. Hahn, and I. Nasser, Phys. Rev. A **38**, 2762 (1988).
[9] V. L. Jacobs, J. Davis, J. E. Rogerson, and M. Blaha, Astrophys. J. **230**, 627 (1979).